Measurement of the Intrinsic Properties of Materials by Time-Domain Techniques

A. M. NICOLSON, MEMBER, IEEE, AND G. F. ROSS, SENIOR MEMBER, IEEE

Abstract—**In this paper a method is presented for determining the complex permittivity and permeability of linear materials in the frequency domain by a single time-domain measurement; typically, the frequency band extends from VHF through X band. The technique described involves placing an unknown sample in a microwave TEM-mode fixture and exciting the sample with a subnanosecond baseband pulse. The fixture is used to facilitate the measurement of the forward- and back-scattered energy, $s_{21}(t)$ and $s_{11}(t)$, respectively. It is shown in this paper that the forward- and back-scattered time-domain "signatures" are uniquely related to the intrinsic properties of the materials, namely, ϵ^* and μ^*. By appropriately interpreting $s_{21}(t)$ and $s_{11}(t)$, one is able to determine the real and imaginary parts of ϵ and μ as a function of frequency. Experimental results are presented describing several familiar materials.**

Introduction

THIS PAPER describes a new method for obtaining the complex permittivity and permeability of linear materials over a broad range of microwave frequencies. Traditionally, such measurements have been made at fixed frequencies in the frequency domain using slotted-line and impedance-bridge configurations [1]. Recently, a technique was described [2] for the measurement of scattering parameters of a broad-band microwave component by obtaining the reflected and transmitted transient responses of the component to an incident subnanosecond risetime pulse and then performing discrete Fourier transforms on the three waveforms. It was pointed out that while the frequency resolution obtainable by this method could not approach that achievable with narrow-band frequency-domain methods, bandwidths of up to two or even three decades could be spanned with a single transient measurement, and the technique was thus best suited to components whose properties changed relatively slowly with frequency. An excellent application of this capability has proved to be that of materials measurements; a system has been developed that spans the range 0.4–10 GHz with 0.4-GHz resolution and yields the complex permittivity and permeability of materials over this range from one pair of transient response measurements. A description of this system is given, and the manner in which its frequency range and accuracy might be further improved is indicated.

Manuscript received June 4, 1970. This work was supported in part by the Air Force Avionics Laboratory Director's Fund, Wright-Patterson Air Force Base, Ohio.

The authors are with the Sperry Rand Research Center, Sudbury, Mass.

Basic Principle

Consider an annular disk of material with permeability $\mu = \mu_0\mu_R$, permittivity $\epsilon = \epsilon_0\epsilon_R$ and thickness d, installed in a coaxial air-filled line with characteristic impedance Z_0 as shown in Fig. 1(a). Within the region $0 \leq x \leq d$ the line will assume a new characteristic impedance $Z = \sqrt{\mu_R/\epsilon_R}\, Z_0$, where μ_R and ϵ_R may be complex. If d were infinite, then the reflection coefficient of a wave incident on the interface from the air-filled line would be given simply by

$$\Gamma = \frac{Z - Z_0}{Z + Z_0} = \frac{\sqrt{\mu_R/\epsilon_R} - 1}{\sqrt{\mu_R/\epsilon_R} + 1}. \tag{1}$$

For finite d, the transmission coefficient between faces A and B of the slab may be written

$$z = \exp -j\omega\sqrt{\mu\epsilon}\, d = \exp\left[-j(\omega/c)\sqrt{\mu_R\epsilon_R}\, d\right]. \tag{2}$$

The scattering coefficients S_{21} and S_{11} of the slab may be obtained from the flow graph, Fig. 1(b), namely,

$$S_{21}(\omega) = \frac{V_B}{V_{\text{inc}}} = \frac{(1 + \Gamma)(1 - \Gamma)z}{1 - \Gamma^2z^2} = \frac{(1 - \Gamma^2)z}{1 - \Gamma^2z^2} \tag{3}$$

$$S_{11}(\omega) = \frac{V_A}{V_{\text{inc}}} = \frac{(1 - z^2)\Gamma}{1 - \Gamma^2z^2}. \tag{4}$$

Writing the sums and differences of the scattering coefficients as

$$\begin{aligned} V_1 &= S_{21} + S_{11} \\ V_2 &= S_{21} - S_{11} \end{aligned} \tag{5}$$

and if

$$X = \frac{1 - V_1V_2}{V_1 - V_2}$$

then it can be shown that Γ may be obtained from the scattering coefficients, since

$$\Gamma = X \pm \sqrt{X^2 - 1} \tag{6}$$

and the appropriate sign is chosen so that $|\Gamma| \leq 1$. Also,

$$z = \frac{V_1 - \Gamma}{1 - V_1\Gamma}. \tag{7}$$

Now from (1) we define

$$\frac{\mu_R}{\epsilon_R} = \left(\frac{1 + \Gamma}{1 - \Gamma}\right)^2 = c_1 \tag{8}$$

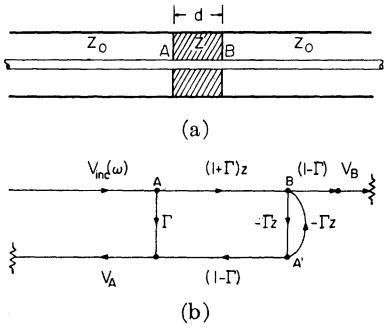

Fig. 1. (a) A coaxial line with annular disk of material to be measured inserted. (b) Signal flow graph for (a).

and from (2) we define

$$\mu_R\epsilon_R = -\left\{\frac{c}{\omega d}\ln\left(\frac{1}{z}\right)\right\}^2 = c_2. \tag{9}$$

Then,

$$\mu_R = \sqrt{c_1c_2}$$
$$\epsilon_R = \sqrt{\frac{c_2}{c_1}}. \tag{10}$$

Complex permeability and permittivity are thus obtained from measurement of the transmission and reflection scattering coefficients of a slab of the material.

Time-Domain Measurement

The above description discussed the use of measurements of S_{21} and S_{11} in the frequency domain, but we are concerned in this paper with the derivation of S_{21} and S_{11} from a time-domain measurement. Measurement of the scattering parameters of microwave networks over broad bandwidths by taking the Fourier transform of the transient response to a subnanosecond pulse has been described previously [2]. Such a method has the advantages of speed and simplicity of the RF part of the measurement system when compared with conventional bridge or slotted-line methods, and in addition can eliminate the mismatch error due to multiple reflections. A computer-controlled broad-band sampling oscilloscope scans and digitizes the transient responses of the microwave sample, and then performs the Fourier transform and subsequent computation to obtain μ_R and ϵ_R.

The configuration used for the measurements is shown in Fig. 2. The pulse from the pulse generator typically has a risetime of less than 100 ps. It propagates down the coaxial delay line, through the feedthrough sampling head of the oscilloscope, and is incident on the sample of material in the test sample holder. The pulse is partially reflected and partially transmitted through the sample. The transmitted pulse reflects from a short circuit, returns up the line, and passes again through the sample on its way to the oscilloscope sampling head. We shall show that these waveforms yield $S_{11}(\omega)$ and $S_{21}^2(\omega)$. The delay-line lengths are chosen sufficiently long so that at the sampling head the incident, reflected, and doubly-transmitted

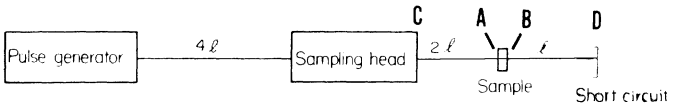

Fig. 2. Time-domain measurement system.

transient-voltage waveforms do not overlap. Consideration of the lengths shown in Fig. 2 will show that the reflected and transmitted waveforms each have a "time-window" over which they may be measured uncontaminated by other reflections of $2l/c$ seconds.

The measurement procedure is as follows. With a short-circuiting metallic plug installed in the coaxial line such that its reflecting face is exactly at position A, the waveform $v_{sc1}(t - t_0)$ is measured over the appropriate time window, where $t_0 = \overline{AC}/c$. Assuming a perfect short circuit, $v_{sc1}(t - t_0) = -v_{inc}(t - t_0)$. With no material in the line, the region d being air filled, the waveform $v_{sc2}(t - t_0 - 2\hat{t}_0 - 2\tau)$ is now measured over an appropriate, somewhat later time window, where $\hat{t}_0 = \overline{BD}/c$ and $\tau = d/c$. Again, assuming a perfect short circuit at D, $v_{sc2}(t - t_0 - 2\hat{t}_0 - 2\tau) = -v_{inc}(t - t_0 - 2\hat{t}_0 - 2\tau)$. The sample is now installed in the line, with its face again at A, and two measurements are made. Over exactly the same time window as for v_{sc1}, we measure the reflected wave $v_A(t - t_0) = v_{inc}(t - t_0)*s_{11}(t)$, where * denotes convolution, $s_{11}(t) \overset{\mathfrak{F}}{\leftrightarrow} S_{11}(\omega)$, and $\mathfrak{F}$ denotes the Fourier transform. Over exactly the same time window as for v_{sc2}, we measure $v_B(t - t_0 - 2\hat{t}_0)*s_{12}(t)$, where $s_{12}(t) \overset{\mathfrak{F}}{\leftrightarrow} S_{12}(\omega)$ and the convolution occurs because of the passage of the transmitted waveform $v_B(t)$ again through the sample. Now $v_B(t - t_0 - 2\hat{t}_0) = v_{inc}(t - t_0 - 2\hat{t}_0)*s_{21}(t)$.

Each of the four measured waveforms is digitized and read into a laboratory computer, and a discrete Fourier transform is performed. By taking the ratios of the appropriate pairs of these transforms, we then obtain

$$\frac{\mathfrak{F}v_A(t - t_0)}{\mathfrak{F}v_{sc1}(t - t_0)} = -\frac{\mathfrak{F}v_{inc}(t - t_0) * s_{11}(t)}{\mathfrak{F}v_{inc}(t - t_0)}$$
$$= -S_{11}(\omega)$$

and

$$\frac{\mathfrak{F}v_B(t - t_0 - 2\hat{t}_0) * s_{12}(t)}{\mathfrak{F}v_{inc}(t - t_0 - 2\hat{t}_0 - 2\tau)}$$
$$= \frac{\mathfrak{F}v_{inc}(t - t_0 - 2\hat{t}_0) * s_{21}(t) * s_{12}(t)}{\exp -j2\omega\tau\,\mathfrak{F}v_{inc}(t - t_0 - 2\hat{t}_0)}$$
$$= S_{21}(\omega)\cdot S_{12}(\omega)\cdot \exp j2\omega\tau.$$

Assuming the sample to be reciprocal, $S_{21}(\omega) = S_{12}(\omega)$. The phase factor in the second expression requires only a knowledge of the sample thickness d. Thus the ratios of the reflected spectra and the transmitted spectra, with the latter multiplied by $\exp -j2\omega\tau$, yield $S_{11}(\omega)$ and $S_{21}^2(\omega)$, respectively. Note that even if the delay lines are not lossless, the transient responses are normalized to effective incident pulses that have traversed the same lengths of line, and no error results.

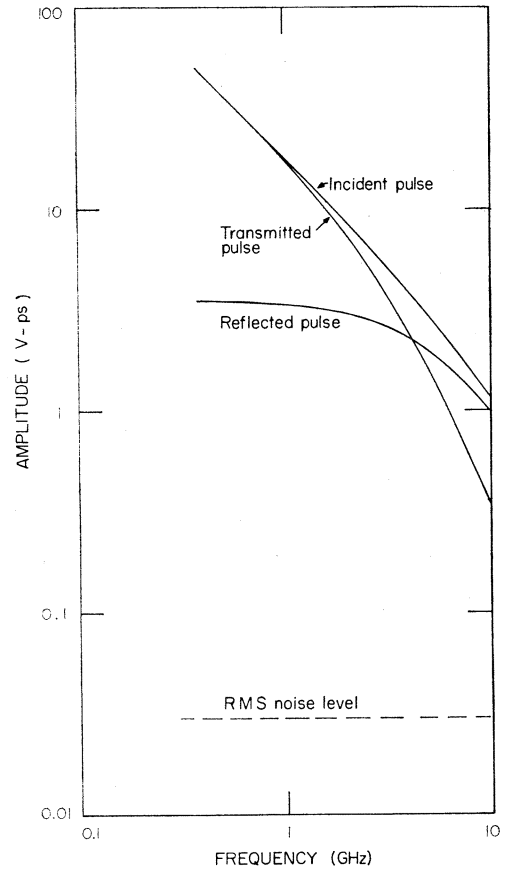

Fig. 3. Typical amplitude spectra for a dielectric with $\epsilon'_R = 15$.

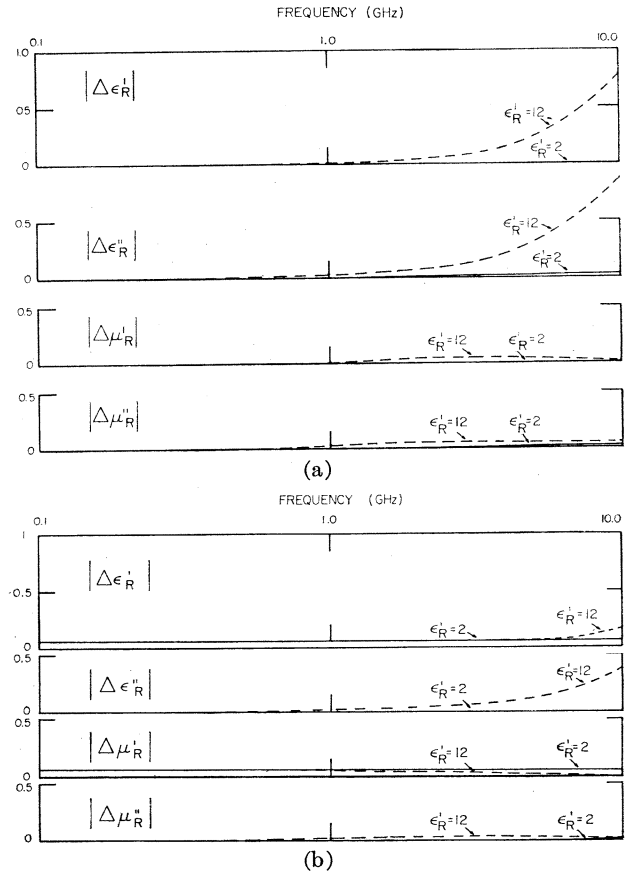

Fig. 4. Errors in ϵ_R and μ_R caused by timing shift of 1 ps in measurement of (a) S_{11} and (b) S^2_{21}.

Discussion of Errors

In approximating the continuous Fourier transform by a discrete Fourier transform, errors arise due to truncation and aliasing [2], [3]. These have been discussed previously and may be reduced by appropriate choice of both the equivalent time interval T between the digitized samples and the total number N of digitized samples. For the results presented here, $T = 9.77$ ps and $N = 256$, giving a time window of 2.5 ns and a fold-over frequency of 51 GHz, which resulted in truncation and aliasing errors becoming small compared with other sources of error.

A major source of error is the relatively low spectral intensity available from subnanosecond risetime pulse generators. The amplitude of the pulse incident on the sample that was used in this study was about 120 mV, with 30 ps risetime. The amplitude spectrum of this pulse, which was long compared to the 2.5-ns window and hence is effectively step-like, is shown in Fig. 3 along with the reflected and doubly transmitted amplitude spectra from a typical dielectric sample. Also shown in the figure is the measured rms noise level in the spectrum; when appropriate steps are taken to remove errors due to drift voltages in the measured waveforms, as will be described later, the oscilloscope amplifier noise spectrum is approximately white, and to this noise is added random errors due to quantization and roundoff in the Fourier transform computation. Because of the $1/f$ spectrum of the incident step-like waveform, the signal/noise ratios of reflected and transmitted spectra fall rapidly as frequency increases, and calculated values for ϵ_R and μ_R become less accurate.

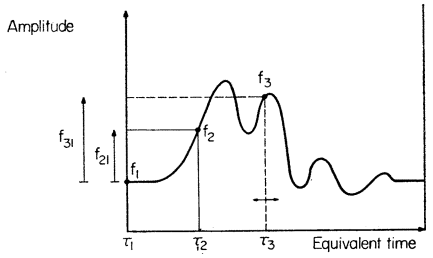

Fig. 5. Principle of three-point scanning of a sampling-oscilloscope waveform.

Another source of error is small timing shifts between the windows used to measure the reflected waveform from a sample, for example, and that from the short circuit that provides its corresponding effective incident waveform ($v_A(t - t_0)$ and $v_{sc1}(t - t_0)$ above). If one window is displaced by an amount Δt relative to the other, then the ratio of Fourier transforms, and hence $S_{11}(\omega)$, will be multiplied by an error exp $j\omega$ Δt. As an example, errors in ϵ_R and μ_R for two samples 0.1 inch thick of dielectric constants $\epsilon'_R = 2.0$ and 12.0, respectively, were calculated, assuming that an error of only $\Delta t = 1$ ps had occurred in S_{11} and S^2_{21} when these were measured. The errors as a function of frequency are shown in Fig. 4. It can be seen that for the higher dielectric constant, even such a small

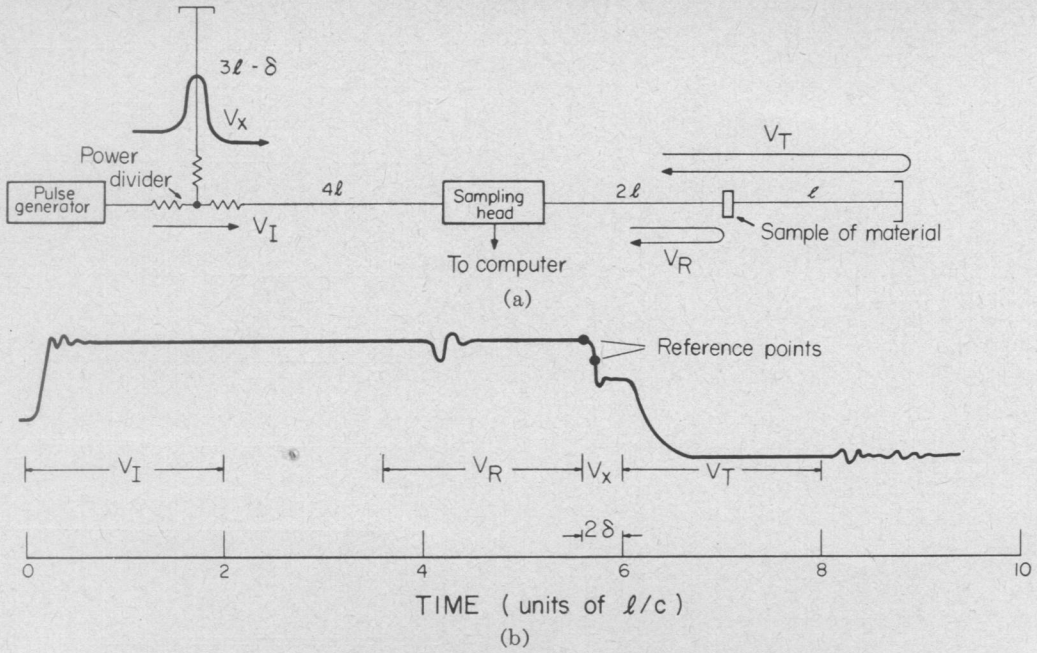

Fig. 6. (a) Final measurement system. (b) Typical waveform.

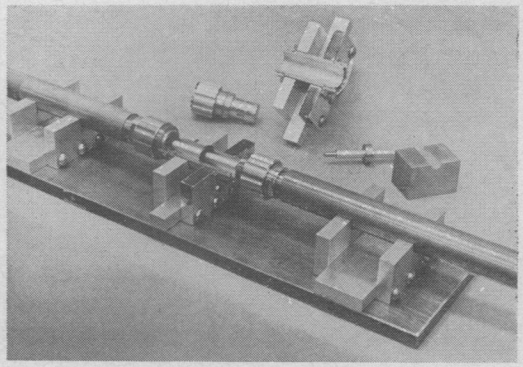

Fig. 7. Sample holder.

timing displacement as 1 ps will cause errors of ± 0.5 in ϵ_R' and ϵ_R'' at frequencies approaching 10 GHz. It has been demonstrated [4] that timing shifts of several picoseconds can occur readily in a broad-band sampling oscilloscope over a period of a few minutes. In addition, such timing shifts could result from linear expansion of the delay lines due to temperature changes. Some form of timing-position stabilization of the 2.5 ns window is required.

A method for simultaneous reduction of additive voltage drift and timing shifts by a technique called three-point scanning has been described [4]. Instead of a sawtooth waveform, the X deflection of the sampling oscilloscope is driven to discrete positions by a small computer integral to the measurement system. With reference to Fig. 5, repeated measurements are made sequentially at three points within the time window. At the fixed first point the waveform slope is zero, at the second fixed point the slope is finite, and the third position incrementally moves across the window. If the three positions are scanned in a time short enough for additive voltage drift and timing shift to be highly correlated, then the difference voltages f_{31} and f_{21} will be independent of additive drift. In addition, changes in f_{21} from an initially recorded value must be due to timing shift. If the slope at point 2 is known, a closed loop may be constructed using the computer so that changes in f_{21} cause corresponding correction voltages to be generated in the scanning circuitry to return point 2, and hence the time window, to its original position. In this way it is possible to reduce long-term timing shifts to less than 1 ps in time windows up to several nanoseconds wide. Successive values of f_{31} are stored as the third point scans across the window.

Results

The final measurement system was that shown in Fig. 6. In order to provide a reference slope for the three-point scanning system mentioned above that did not alter position as the samples were removed and inserted, a short-circuited stub and power divider were added as shown. The voltage ramp resulting from this stub was adjusted to occur just between the end of the reflected-voltage time window and the beginning of the transmitted-voltage time window.

The coaxial delay lines and sample holder were constructed with 9/16-inch-diameter air-filled line and General Radio GR900 precision connectors. The sample holder is shown in Fig. 7, and was constructed from a 2-inch length of air-dielectric line cut longitudinally. The inner conductor for this section had spring-loaded locating pins at each end. In this way the samples could be inserted by sliding the lines apart only about an inch at the sample holder, and the samples could be positioned accurately in the holder by use of a gauge block, which can also be seen in Fig. 7. An error of 0.005 inch in the position of the sample can contribute 1 ps timing-shift error in the measurement of $S_{11}(\omega)$.

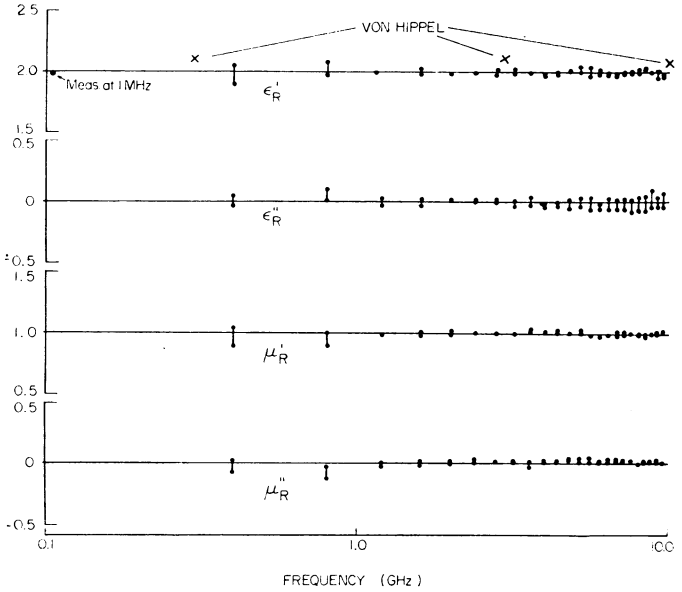

Fig. 8. 1_R and ϵ_R for Teflon, 0.25 inch thick.

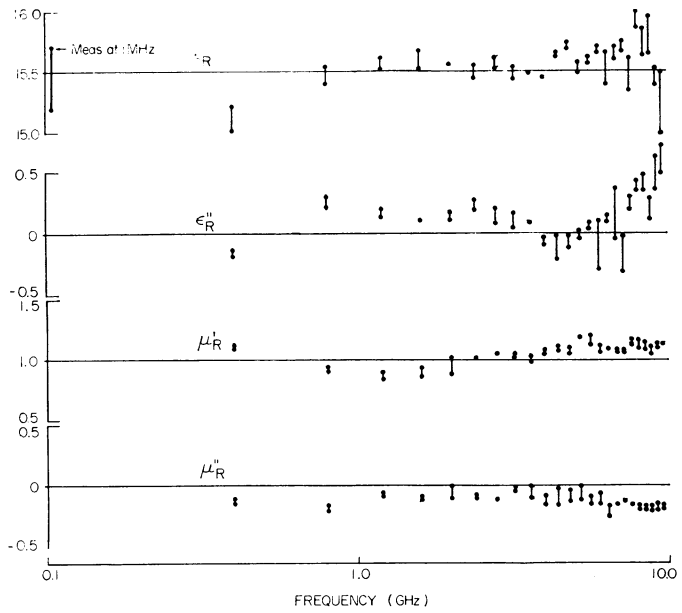

Fig. 9. μ_R and ϵ_R for dielectric with $\epsilon'_R = 15$, 0.05 inch thick.

Some filtering that reduces noise occurs between the sampling oscilloscope amplifier output and the analog–digital converter in the computer. In addition, further noise reduction is obtained by recording and averaging four 256-point scans of each waveform. Since each set of four scans occupied about 7 minutes, after the initial reference waveforms had been acquired each sample required about 15 minutes to measure. Subsequent 256-point fast Fourier transforms and other computations occupy about another 5–10 minutes for each sample.

Typical results are shown in Figs. 8–12. A sample of Teflon 0.25 inch thick was measured on separate occasions, and the reproducibility of the results may be seen in Fig. 8 for the frequency range 0.4–9.6 GHz. Also shown is a mesaurement on the same sample at

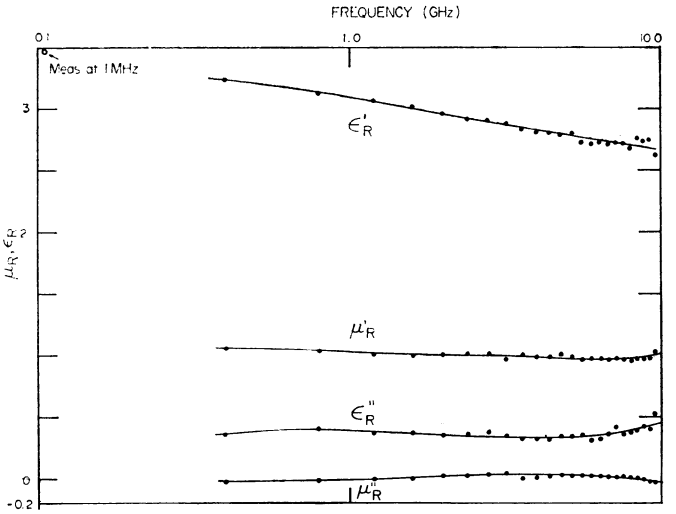

Fig. 10. μ_R and ϵ_R for wood (maple), 0.25 inch thick.

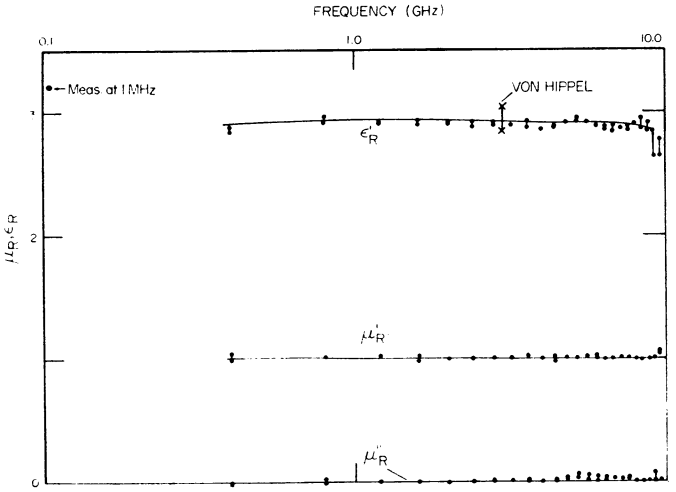

Fig. 11. μ_R and ϵ_R for nylon, 0.25 inch thick.

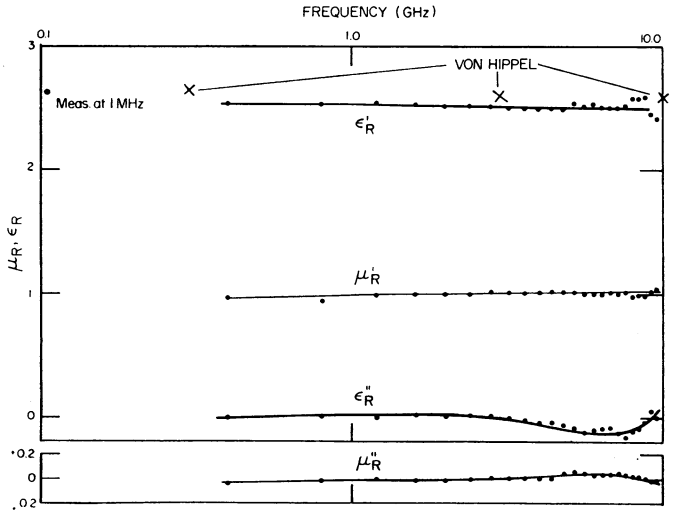

Fig. 12. μ_R and ϵ_R for Plexiglas, 0.25 inch thick.

1 MHz in a parallel-plate capacitance bridge and the values quoted by von Hippel [1]. Reproducibility is within ±0.1 over the range of frequencies for ϵ_R', ϵ_R'', μ_R', and μ_R''.

Measurements on two samples of a dielectric material with $\epsilon_R' \approx 15$, 0.05 inch thick, are shown in Fig. 9, again compared with 1-MHz measurements. Reproducibility is now about ±0.5 over the range of frequencies, differences in ϵ_R' and ϵ_R'' being somewhat greater than those for μ_R' and μ_R''. An example of a lossy material is shown in Fig. 10 for a maple-wood sample; the increased value of ϵ_R'' is seen clearly. Measurements on nylon and Plexiglas are shown in Figs. 11 and 12, again compared with 1-MHz values and those quoted by von Hippel.

Conclusions

A method has been demonstrated for measurement of the complex permeability and permittivity of materials over broad frequency ranges from their time-domain transient response. Repeatability is within ±0.1 for permeabilities and permittivities of around 2–3, the bound increasing to perhaps ±0.5 for permittivities of 12–15. Further work on this technique might concentrate on the use of longer delay lines to increase the available time windows, and hence increase frequency resolution. Some compromise is necessary, since the attenuation due to skin effect in longer lines will reduce the higher frequency components of the incident pulse. Improved pulse-generator design to produce greater spectral intensity at frequencies near 10 GHz could also offer significant improvement.

References

[1] A. R. von Hippel, Ed., *Dielectric Materials and Applications*. New York: Wiley, 1961.
[2] A. M. Nicolson, "Broad-band microwave transmission characteristics from a single measurement of the transient response," *IEEE Trans. Instrum. Meas.*, vol. IM-17, pp. 395–402, December 1968.
[3] G. D. Bergland, "A guided tour of the fast Fourier transform," *IEEE Spectrum*, vol. 6, pp. 41–52, July 1969.
[4] A. M. Nicolson, "Wideband system function analyzer employing time to frequency domain translation," presented at WESCON, San Francisco, Calif., August 1969.

Generation of Reference Waveforms by Uniform Lossy Transmission Lines

W. D. McCAA, JR., MEMBER, IEEE, AND NORRIS S. NAHMAN, SENIOR MEMBER, IEEE

***Abstract*—This paper describes a method for generating fractional nanosecond pulsed waveforms of known shape thereby providing an a priori means for establishing reference waveform generators or standards to be used in pulsed measurements and other applications. The method employs the band-limiting properties of a lossy uniform transmission line to produce a known waveform and generator impedance. A theory for generator characterization and application is presented that defines a given generator in terms of time-domain or frequency-domain functions. A new term called the "available" waveform is defined. Rms error is employed as the error criteria.**

An example of generator design is given that employs planar skin-effect loss and provides an output response having 0.2 percent rms error over the interval $0 \leq t \leq 600$ ps referred to the inherent step response of the waveshaping line. The input transition generator is assumed to be a 30-ps unit ramp generator. Also, an application example is given that employs a reference waveform generator to evaluate a sampling oscilloscope. The reference waveform generator uses a Debye dielectric lossy transmission line. The rms error of the oscilloscope time-domain response is determined as a function of time.

Manuscript received June 25, 1970.
The authors are with the Electromagnetics Division, National Bureau of Standards, Boulder, Colo. 80302.

Introduction

THE objectives of this paper are to present the theory for the generation of reference waveforms using uniform lossy transmission lines and to provide some examples of generators and applications. The paper is organized into four sections: generator characterization, intrinsic loss waveforms, generator design, and reference-waveform application.

I. Generator Characterization

In theoretical time-domain studies the ideal-unit step generator or the ideal-unit impulse generator is commonly used as a driving source. However, in experimental work either of these ideal generators is necessarily replaced by a physically realizable one, i.e., a transition generator or an impulsive generator.